Received: 14 June 2021 | Revised: 1 October 2021 | Accepted: 13 October 2021

DOI: 10.1002/hep.32221

ORIGINAL ARTICLE

Breviscapine alleviates NASH by inhibiting TGF-β-activated kinase 1-dependent signaling

Tian Lan[1,2,3,4] | Shuo Jiang[1,2,3,4] | Jing Zhang[1,2,3,4] | Qiqing Weng[1,2,3,4] | Yang Yu[1,2,3,4] | Haonan Li[1,2,3,4] | Song Tian[5] | Xin Ding[1,2,3,4] | Sha Hu[5] | Yiqi Yang[1,2,3,4] | Weixuan Wang[1,2,3,4] | Lexun Wang[1,2,3,4] | Duosheng Luo[1,2,3,4] | Xue Xiao[1,2,3,4] | Shenghua Piao[1,2,3,4] | Qing Zhu[1,2,3,4] | Xianglu Rong[1,2,3,4] | Jiao Guo[1,2,3,4]

[1]Institute of Chinese Medicine, Guangdong Pharmaceutical University, Guangzhou, China

[2]Guangdong Metabolic Diseases Research Center of Integrated Chinese and Western Medicine, Guangzhou, China

[3]Key Laboratory of Glucolipid Metabolic Disorder, Ministry of Education, Guangzhou, China

[4]Guangdong TCM Key Laboratory for Metabolic Diseases, Guangzhou, China

[5]Department of Cardiology, Renmin Hospital of Wuhan University, Wuhan, China

Correspondence
Jiao Guo, Guangdong Pharmaceutical University, Guangzhou Higher Education Mega Center, 280 Wai Huan Dong Road, Guangzhou 510006, China.
Email: gyguoyz@163.com

Funding information
The Special Topics of General Projects of Guangzhou Science and Technology Plan of China, Grant/Award Number: 201904010075; the Major Basic and Applied Basic Research Projects in Guangdong Province of China, Grant/Award Number: 2019B030302005; the National Natural Science Foundation of

Abstract

Background and Aims: NAFLD is a key component of metabolic syndrome, ranging from nonalcoholic fatty liver to NASH, and is now becoming the leading cause of cirrhosis and HCC worldwide. However, due to the complex and unclear pathophysiological mechanism, there are no specific approved agents for treating NASH. Breviscapine, a natural flavonoid prescription drug isolated from the traditional Chinese herb *Erigeron breviscapus*, exhibits a wide range of pharmacological properties, including effects on metabolism. However, the anti-NASH efficacy and mechanisms of breviscapine have not yet been characterized.

Approach and Results: We evaluated the effects of breviscapine on the development of hepatic steatosis, inflammation, and fibrosis *in vivo* and *in vitro* under metabolic stress. Breviscapine treatment significantly reduced lipid accumulation, inflammatory cell infiltration, liver injury, and fibrosis in mice fed a high-fat diet, a high-fat/high-cholesterol diet, or a methionine- and choline-deficient diet. In addition, breviscapine attenuated lipid accumulation, inflammation, and lipotoxicity in hepatocytes undergoing metabolic stress. RNA-sequencing and multiomics analyses further indicated that the

Abbreviations: Accα, acetyl CoA carboxylase alpha; Actb, actin beta; ALT, alanine aminotransferase; AST, aspartate aminotransferase; Ccl2/5, C-C motif chemokine ligand 2/5; Col1a1/3a1, collagen type I/III alpha 1; Cpt1α, carnitine palmitoyltransferase 1a, liver; Ctgf, connective tissue growth factor; Cxcl2/10, C-X-C motif chemokine ligand 2/10; Fabp1, fatty acid binding protein 1; FASN, fatty acid synthase; GAPDH, glyceraldehyde 3-phosphate dehydrogenase; GSEA, gene set enrichment analysis; GSVA, gene set variation analysis; H&E, hematoxylin and eosin; HFD, high-fat diet; HFHC, high-fat/high-cholesterol; IKBα, inhibitor of kappa light polypeptide gene enhancer in B cells alpha; IKKβ, inhibitor of NF-κB kinase subunit beta; JNK, c-Jun N-terminal kinase; KEGG, Kyoto Encyclopedia of Genes and Genomes; LW, liver weight; LW/BW, liver weight-to-body weight ratio; MAPK, mitogen-activated protein kinase; MCD, methionine- and choline-deficient; MCS, methionine- and choline-sufficient; NC, normal chow; OA, oleic acid; p-, phosphorylated; PA, palmitic acid; PCA, principal component analysis; PO, PA + OA; Pparα/γ, peroxisome proliferator-activated receptor α/γ; PPI, protein–protein interaction; PSR, picrosirius red; RNA-seq, RNA sequencing; SCD1, stearoyl-CoA desaturase 1; TAK1, TGF-β-activated kinase 1; TC, total cholesterol; TG, triglyceride; Timp1, tissue inhibitor of metalloproteinase 1.

Tian Lan, Shuo Jiang, Jing Zhang, and Qiqing Weng are contributed equally to this work.

China, Grant/Award Number: 81830113, 81870420 and 82070590; the National Key R & D Plan of China "Research on Modernization of Traditional Chinese Medicine" program, Grant/Award Number: 2018YFC1704200

key mechanism linking the anti-NASH effects of breviscapine was inhibition of TGF-β-activated kinase 1 (TAK1) phosphorylation and the subsequent mitogen-activated protein kinase signaling cascade. Treatment with the TAK1 inhibitor 5Z-7-oxozeaenol abrogated breviscapine-mediated hepatoprotection under metabolic stress. Molecular docking illustrated that breviscapine directly bound to TAK1.

Conclusion: Breviscapine prevents metabolic stress–induced NASH progression through direct inhibition of TAK1 signaling. Breviscapine might be a therapeutic candidate for the treatment of NASH.

INTRODUCTION

NAFLD is a major global health problem that is considered to be a chronic hepatic manifestation of metabolic syndrome, ranging from steatosis to steatohepatitis and liver fibrosis.[1,2] NASH is a severe form of NAFLD and a risk factor for cirrhosis and HCC.[3] Steatosis, hepatocyte injury, inflammation, and various degrees of fibrosis are recognized as important components in the pathogenesis of NASH.[4] However, there is currently no effective pharmacological therapy approved for NASH, and efforts to control complications arising from the condition are far from satisfactory.[5] Therefore, approaches for developing promising treatment strategies for this highly prevalent disease are urgently needed.

Breviscapine, as a prescription drug, is a flavonoid extract from the traditional Chinese herb *Erigeron breviscapus* (Vant.) Hand.-Mazz, whose main ingredient is scutellarin (≥90%).[6] At present, more than 10 million patients use breviscapine and related drugs each year in China.[7] Owing to its multiple pharmacological activities, including anti-inflammatory, antioxidative, antiapoptotic, vasorelaxant, antiplatelet, anticoagulation, and myocardial protective activities, breviscapine has been widely used to treat cerebrovascular disease, cardiovascular disease, and diabetic complications.[8] Recent studies have demonstrated that breviscapine protects against CCl_4-induced liver injury by reducing proinflammatory cytokine secretion and oxidative stress.[9] Furthermore, scutellarin, the main component of breviscapine, has been shown to regulate lipid metabolism and may exhibit useful therapeutic effects against NAFLD by reducing oxidative stress.[10,11] However, whether breviscapine prevents NASH and its underlying mechanism are not yet clear.

The present study was designed to determine the effects of breviscapine on the pathogenesis of NASH, including its impacts on lipid accumulation, hepatic injury, inflammation, and fibrosis. We found that breviscapine attenuated hepatic lipid accumulation, inflammation, and fibrosis in mice fed a high-fat diet (HFD), a high-fat/high-cholesterol (HFHC) diet, or a methionine- and choline-deficient (MCD) diet, individually. Mechanistically, our data identify breviscapine as a promising candidate for the treatment of NASH whose effects are mediated by direct inhibition of TGF-β-activated kinase 1 (TAK1).

MATERIALS AND METHODS

Animals and treatments

Healthy 8- to 10-week-old male *C57BL/6J* mice were housed in cages under standard laboratory conditions (22–24°C temperature, 55%–60% relative humidity, and 12 h light/dark cycle). A mouse model of NASH was established by feeding the mice an HFHC (protein, 14%; fat, 42%; carbohydrates, 44%; cholesterol, 2%; IMA2019001; TrophicDiet, Nantong, China) diet for 16 weeks, and breviscapine (15 and 30 mg/kg) (190620, Shanghai Winherb Medical Science Co., Ltd., Shanghai, China) was administered daily by oral gavage after 8 weeks. The animal experiments were approved by the Institutional Animal Care and Use Committee of Renmin Hospital of Wuhan University according to the *Guide for the Care and Use of Laboratory Animals* prepared by the National Academy of Sciences and published by the National Institutes of Health. All mice received humane care.

RNA-sequencing analysis

Total RNA was isolated using TRIzol reagent (T9424; Sigma-Aldrich, St. Louis, MO), and the integrity of the RNA was assessed with agarose electrophoresis and an RNA 6000 Nano Kit (5067-1511; Agilent). For RNA sequencing (RNA-seq), complementary DNA libraries were created using the MGIEasy RNA Library Prep Kit (1000006384; MGI, Shenzhen, China) according to the manufacturer's instructions. The single-ended library was sequenced using a BGISEQ-500 instrument (MGI), and the read length was 50 bp. The reads were mapped to the Ensembl human (hg38/GRCh38) and mouse (mm10/GRCm38) reference genomes

with HISAT2 (version 2.1.0) software. Then, SAMtools (version 1.4) was used to convert the files obtained in the above steps into a binary BAM format that could store the comparison information. Next, the fragments per kilobase of exon per million mapped fragments value for each identified gene was calculated using the default parameters of StringTie (version 1.3.3b). Differentially expressed genes (DEGs) were identified with DESeq2 (version 1.2.10) according to the following two criteria: (1) a fold change >1.5 and (2) a corrected p value < 0.05. Finally, the ggplot2 package was used to create a volcano plot showing the fold changes and p values of all genes. The data have been submitted to Sequence ReadArchive (SRA) database with PRJNA number PRJNA781787 and PRJNA782086.

Principal component analysis

Principal component analysis (PCA) was used to compare the differences between the two groups. PCA was implemented using the fast.prcomp function of the R language and then visualized with the ggplot2 package.

Kyoto Encyclopedia of Genes and Genomes pathway enrichment analysis

The Kyoto Encyclopedia of Genes and Genomes (KEGG) is a comprehensive database that integrates genomic, chemical, and system functional information. KEGG pathway enrichment analysis was performed using Fisher's exact test with our in-house R script, and the KEGG pathway annotations for all genes in the selected genome were downloaded from the KEGG database. Pathways with $p < 0.05$ were considered significantly enriched.

Gene set variation analysis

Gene set variation analysis (GSVA) was executed using the GSVA R package (version 1.32.0). For each KEGG pathway, a gene set based on the proteins detected in proteomic analysis was generated. Then, the gene expression matrix of the KEGG pathway was used to calculate the single-sample GSVA scores.

Gene set enrichment analysis

Gene set enrichment analysis (GSEA) was executed on the Java GSEA platform (version 3.0) using the Signal2Noise metric. The genes involved in each KEGG biological pathway were treated as a gene set, and then a ranked list and a gene set permutation of the gene set were generated. Gene sets with $p < 0.05$ and false discovery rate values < 0.25 were considered statistically significant.

Proteomic analysis

Proteomic analysis was performed using mass spectrometry in data-dependent acquisition mode. The abundance of peptide fractions in the control group and the treatment group was quantified using unlabeled quantitative methods, and the difference in the abundance of phosphorylated peptide fractions between the control group and the treatment group was tested for significance by t test. The screening criterion for differentially expressed proteins was $p < 0.05$. The data have been submitted to NCBI PRIDE database with PXD number PXD029867.

Phosphoproteomic analysis

Phosphorylated polypeptides from cell or tissue lysates were enriched with TiO_2 magnetic beads and analyzed by liquid chromatography-tandem mass spectrometry with a Proxeon Easy-NLC 1000 (Thermo Scientific, Shanghai Applied Protein Technology Co., Ltd., Shanghai, China). The abundance of phosphorylated peptides in the control group and the treatment group was quantified using an unlabeled quantitative method, and the difference in the abundance of phosphorylated peptide fractions between the control group and the treatment group was tested for significance by t test. The screening criterion for differentially expressed phosphorylated proteins was $p < 0.05$. The data have been submitted to NCBI PRIDE database with PXD number PXD029975.

The detailed materials and methods are provided in the Supporting Information.

RESULTS

Breviscapine attenuates HFD-induced hepatic injury and metabolic disorders in mice

To examine the pharmacological effects of breviscapine on the hepatic steatosis and injury, we used an HFD-induced obesity mouse model that destroys the balance between the synthesis and degradation of lipids, which results in lipid accumulation and toxicity in hepatocytes. Mice were fed an HFD for 16 weeks and then administered breviscapine intragastrically (15 and 30 mg/kg/day) for an additional 8 weeks with continuous HFD feeding (Figure 1A). During the whole process of the experiment, the body weight of the HFD-fed mice (control-HFD mice) was significantly higher than that of the normal chow (NC)–fed control mice (control-NC mice),

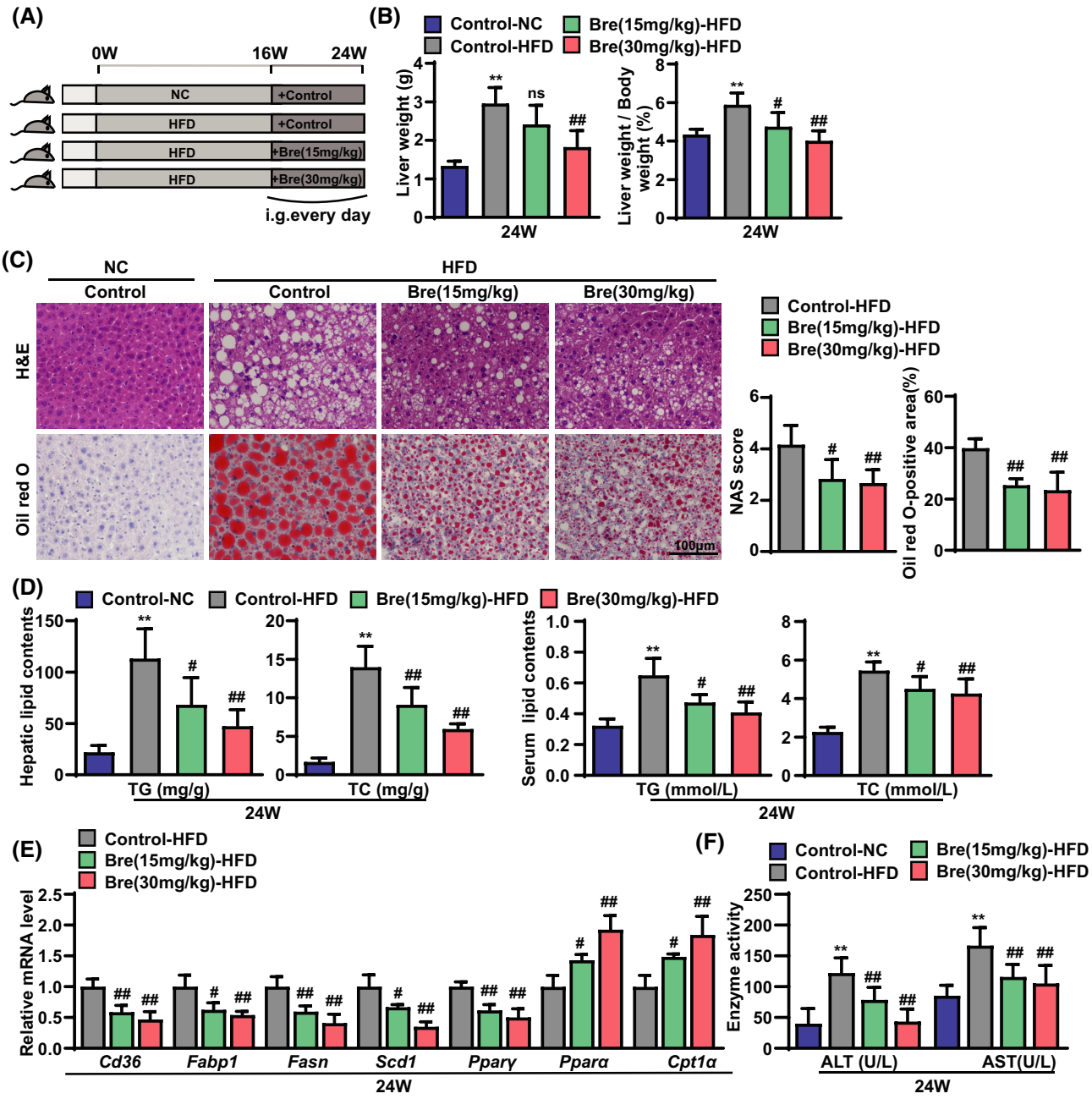

FIGURE 1 Breviscapine alleviates hepatic steatosis and injury in mice fed the HFD. (A) Schematic diagram of the experimental procedure used to examine the protective role of breviscapine in mice fed the NC diet or the HFD for 24 weeks. HFD-fed mice were intragastrically administered saline or breviscapine (15 or 30 mg/kg) once daily beginning at week 16 for 8 weeks. *n* = 8 per group. (B) LW and LW/BW values of mice. *n* = 8 per group. (C) Representative images of H&E and oil red O staining of liver sections from mice. NAFLD activity score and the statistics of oil red O–positive areas are shown. *n* = 6 per group. Scale bar, 100 μm. (D) Lipid (TG and TC) levels in the liver and serum. *n* = 8 per group. (E) Quantitative PCR was performed to determine the hepatic mRNA levels of genes related to fatty acid metabolism (*Cd36, Fabp1, Fasn, Scd1, Pparγ, Pparα,* and *Cpt1a*) in mice from the indicated groups. Gene expression was normalized to actin beta (*Actb*) mRNA levels. *n* = 4–6 per group. (F) Serum levels of ALT and AST were measured in mice after 24 weeks of NC diet feeding or HFD challenge. *n* = 8 per group. The data are presented as the mean ± SD. Significant difference between the control-NC group and the control-HFD group, $^{*}p < 0.05$, $^{**}p < 0.01$; significant difference between the control-HFD group and the Bre-HFD group, $^{\#}p < 0.05$, $^{\#\#}p < 0.01$. The data were analyzed with one-way ANOVA. Abbreviations: Bre, breviscapine; i.g., intragastric administration; NAS, NAFLD activity score; ns, no significant difference between the control-HFD group and the Bre-HFD group

while there were no differences between breviscapine-treated mice and HFD-fed mice (Figure S1A). The increased liver weight (LW) and LW-to-body weight ratio (LW/BW) in HFD-fed mice was remarkably decreased by breviscapine (Figure 1B). In addition, hematoxylin and eosin (H&E) staining and oil red O staining showed

that lipid accumulation in HFD-fed mice was significantly reduced by breviscapine (Figure 1C), which was supported by the liver and serum triglyceride (TG) and total cholesterol (TC) levels (Figure 1D). Additionally, reduced hepatocyte ballooning was observed in mice treated with breviscapine (Figure 1C). Quantitative PCR assays showed that hepatic mRNA levels of genes related to fatty acid uptake and synthesis (*Cd36*, fatty acid binding protein 1 [*Fabp1*], fatty acid synthase [*Fasn*], stearoyl CoA desaturase 1 [*Scd1*], and peroxisome proliferator–activated receptor γ [*Pparγ*]) were significantly diminished by breviscapine treatment. Moreover, the mRNA levels of lipid β-oxidation genes (*Pparα* and carnitine palmitoyltransferase 1a [*Cpt1α*]) were increased in breviscapine-treated mice (Figure 1E). Western blot assays also confirmed that the up-regulation of adipogenic genes (FASN and PPARγ) in HFD-fed mice was significantly abolished by breviscapine (Figure S1B). The serum levels of alanine aminotransferase (ALT) and aspartate aminotransferase (AST) were lower in breviscapine-treated mice than in control-HFD mice (Figure 1F). These results suggest that breviscapine protects mice from hepatic steatosis and injury induced by metabolic stress.

Breviscapine attenuates HFHC diet–induced steatohepatitis

To further assess the potential benefit of breviscapine treatment against the progression of NASH, we next tested the effect of breviscapine in an HFHC diet–induced NASH mouse model. HFHC diet feeding induced more severe hepatic steatosis, inflammation, and fibrosis than HFD feeding, eventually leading to steatohepatitis with features similar to the pathological features of human NASH.[12] Mice were fed an HFHC diet for 8 weeks and then treated with breviscapine (15 and 30 mg/kg/day) by oral gavage with continuous HFHC diet feeding for another 8 weeks (Figure 2A). The LW and the LW/BW of breviscapine-treated mice fed the HFHC diet were lower than those of the control HFHC diet–fed mice (Figure 2B). However, there was no difference in body weight after breviscapine treatment (Figure S2A). Histological examination of liver sections showed that breviscapine treatment significantly improved liver histology, resulting in less hepatic steatosis, ballooning degeneration, and inflammatory cell infiltration in treated mice than in control-HFHC mice (Figure 2C). Consistently, hepatic and serum lipid levels were significantly decreased in breviscapine-treated mice (Figure 2D). Moreover, breviscapine treatment strikingly decreased the mRNA levels of fatty acid uptake–related and synthesis-related genes (*Cd36*, *Fabp1*, *Fasn*, *Scd1*, and *Pparγ*) (Figure 2E) and alleviated the abnormal protein expression of FASN and PPARγ (Figure S2B) in mice fed the HFHC diet. Additionally, the mRNA levels of β-oxidation genes (*Pparα* and *Cpt1α*) were notably increased in breviscapine-treated mice compared to control HFHC mice (Figure 2E). Furthermore, the serum levels of ALT and AST in mice fed the HFHC diet were significantly reduced by breviscapine treatment (Figure 2F).

Liver inflammation and fibrosis exacerbate NASH progression.[13] Next, we examined the effects of breviscapine on NASH-associated inflammation and fibrosis. Immunofluorescence staining of the macrophage marker CD11b showed markedly less macrophage infiltration in liver sections from breviscapine-treated mice than in those from control-HFHC mice (Figure 3A). Quantitative PCR assays showed that breviscapine significantly reduced the mRNA levels of proinflammatory genes (C-C motif chemokine ligands 2 and 5 [*Ccl2*, *Ccl5*], C-X-C motif chemokine ligands 2 and 10 [*Cxcl2*, *Cxcl10*], and *Tnfα*) (Figure 3B). Furthermore, breviscapine treatment significantly down-regulated the hepatic expression of phosphorylated inhibitor of NF-κB kinase subunit beta (p-IKKβ) and nuclear p-p65 in mice fed the HFHC diet, whereas it up-regulated the expression of inhibitor of kappa light polypeptide gene enhancer in B cells alpha (IKBα; Figure 3C). We next measured the effect of breviscapine on NASH-associated fibrosis in mice fed the HFHC diet. Picrosirius red (PSR) staining showed less collagen deposition in the liver sections of breviscapine-treated mice than in those of control HFHC mice (Figure 3D). Additionally, quantitative PCR assays confirmed that breviscapine treatment significantly decreased the hepatic mRNA levels of profibrotic genes (collagen type I/III alpha 1 [*Col1a1*, *Col3a1*], connective tissue growth factor (*Ctgf*), and tissue inhibitor of metalloproteinase 1 [*Timp1*]) in mice fed the HFHC diet (Figure 3E). These results indicate that breviscapine ameliorates HFHC diet–induced steatohepatitis in mice.

Breviscapine attenuates MCD diet–induced steatohepatitis

To further verify the effect of breviscapine on steatohepatitis, another mouse steatohepatitis model induced by MCD diet feeding for 4 weeks was employed.[14] MCD diet–fed mice were administered breviscapine (30 mg/kg) daily for the entire experimental duration (Figure 4A). Consistent with the results obtained with the HFHC mouse model, serum levels of ALT and AST were significantly reduced by breviscapine treatment (Figure 4B). Hepatic TG content was lower in breviscapine-treated mice than in control-MCD mice (Figure 4C). Moreover, H&E staining and oil red O staining showed that breviscapine-treated mice had less severe steatosis and inflammatory cell infiltration than control-MCD mice (Figure 4D). Additionally, CD11b

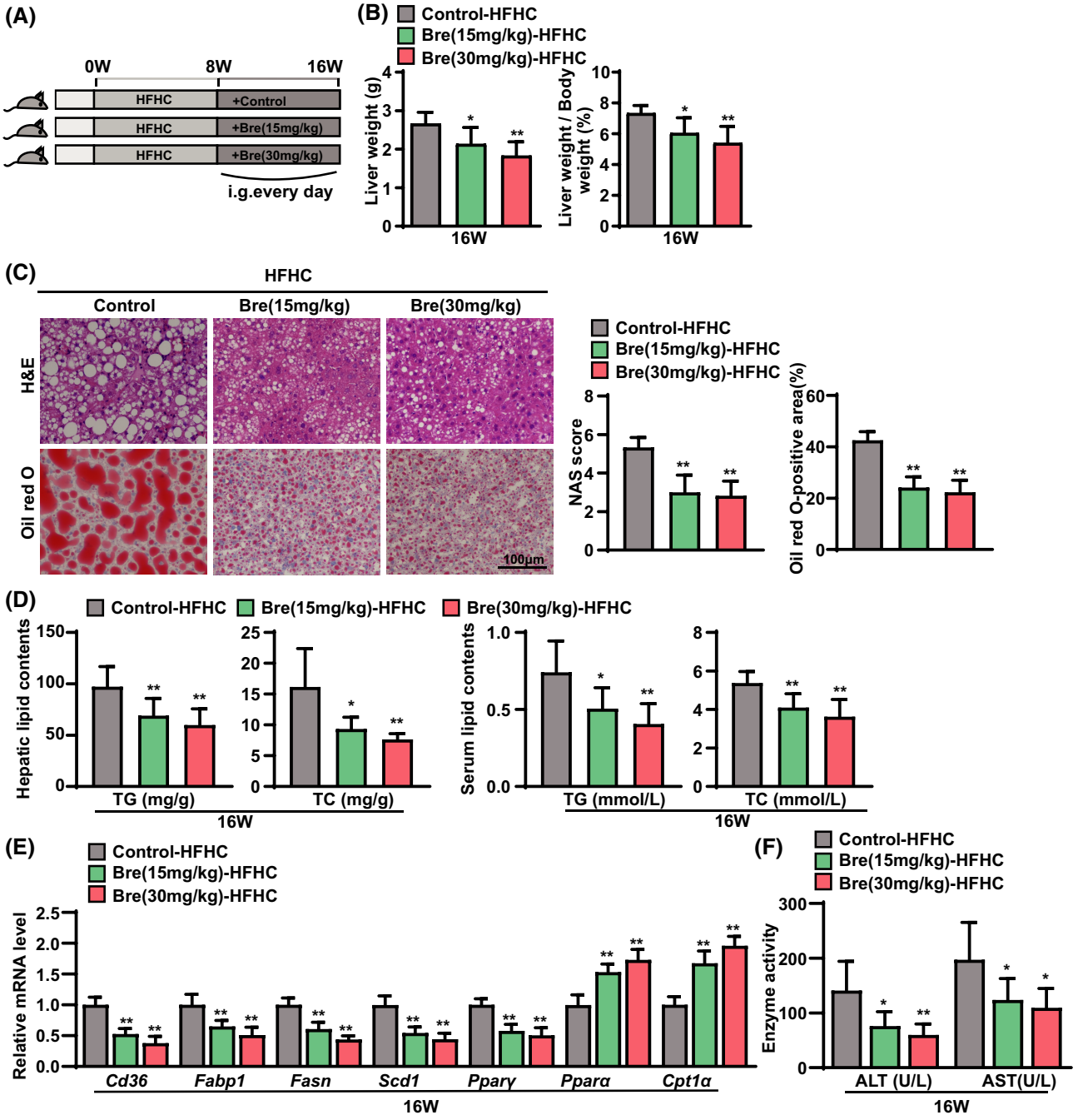

FIGURE 2 Breviscapine represses hepatic steatosis and injury in mice fed an HFHC diet. (A) Schematic diagram of the experimental procedure used to examine the protective effects of breviscapine in mice fed NC or the HFHC diet for 16 weeks. HFHC-fed mice were intragastrically administered saline or breviscapine (15 or 30 mg/kg) once daily beginning at week 8 for 8 weeks. *n* = 9 per group. (B) LW and LW/BW values of mice. *n* = 9 per group. (C) Representative images of H&E and oil red O staining of liver sections from mice. NAFLS activity scores and the statistics of oil red O–positive areas are shown. *n* = 6 per group. Scale bar, 100 μm. (D) Lipid (TG and TC) levels in the liver and serum. *n* = 9 per group. (E) Quantitative PCR was performed to determine the hepatic mRNA levels of genes related to fatty acid metabolism (*Cd36*, *Fabp1*, *Fasn*, *Scd1*, *Pparγ*, *Pparα*, and *Cpt1a*) in mice from the indicated groups. Gene expression was normalized to *Actb* mRNA levels. *n* = 6 per group. (F) Serum levels of ALT and AST were measured in mice after 16 weeks of HFHC challenge. *n* = 9 per group. The data are presented as the mean ± SD. Significant difference between the control-HFHC group and the Bre-HFHC group, **p* < 0.05, ***p* < 0.01. The data were analyzed with one-way ANOVA. Abbreviations: Bre, breviscapine; i.g., intragastric administration; NAS, NAFLD activity score

and PSR staining showed that MCD-induced hepatic inflammation and collagen deposition were abolished by breviscapine treatment (Figure 4E). Quantitative PCR assays also confirmed that breviscapine decreased the mRNA levels of genes related to inflammation (*Ccl2*, *Cxcl2*, and *Tnfα*) and fibrosis (*Col1a1*, *Col3a1*, and *Ctgf*) (Figure 4F). These data further confirm that breviscapine protects mice against experimental steatohepatitis.

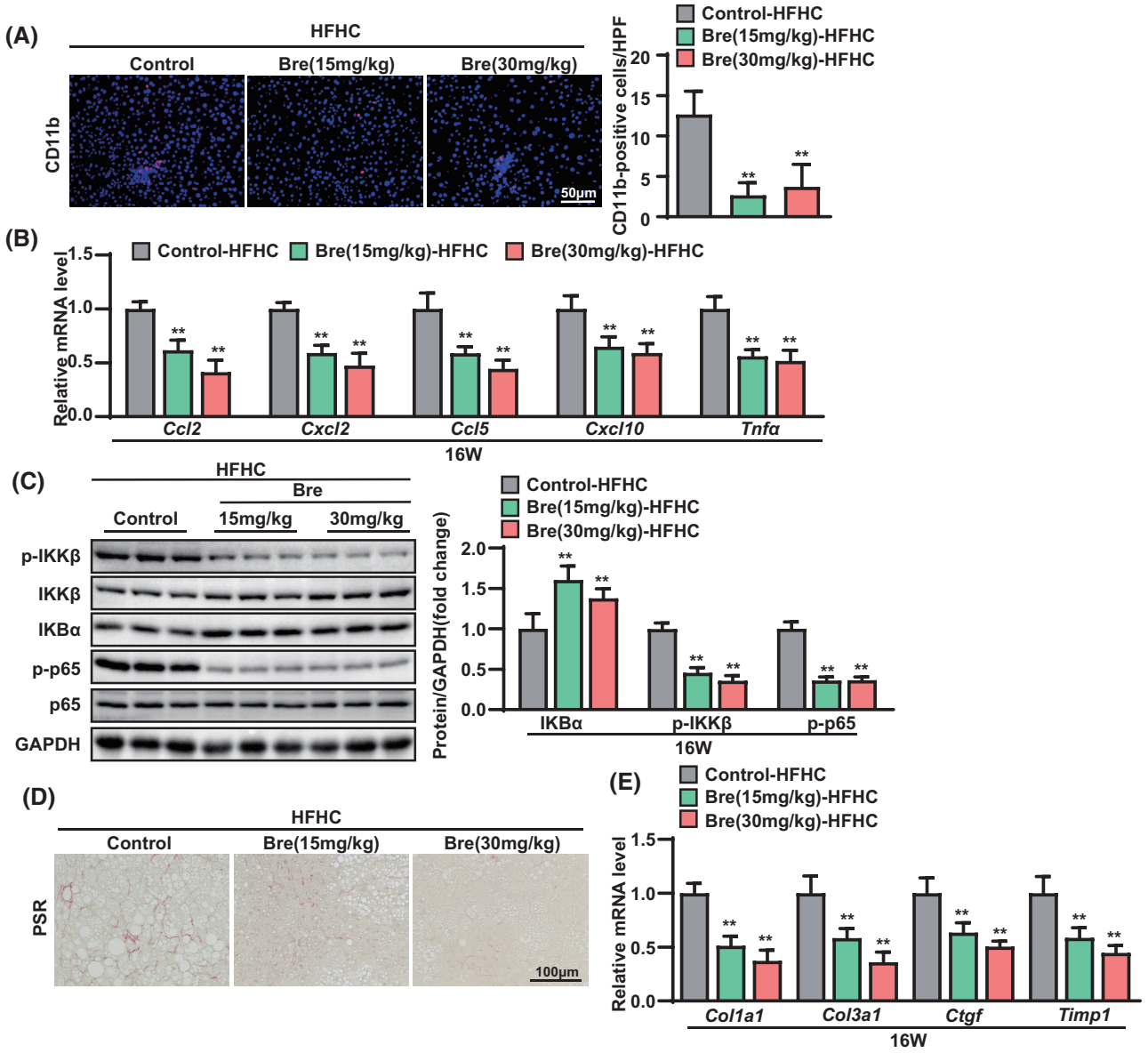

FIGURE 3 Breviscapine attenuates hepatic inflammation and fibrosis in mice fed an HFHC diet. (A) Immunofluorescence staining of CD11b (in red) in the livers of HFHC-fed mice. Nuclei were labeled with DAPI (in blue). The ratios of the numbers of CD11b-positive cells are shown. n = 3–4 per group. Scale bar, 50 μm. (B) Quantitative PCR was performed to determine hepatic mRNA levels of genes related to inflammation (*Ccl2*, *Cxcl2*, *Ccl5*, *Cxcl10*, and *Tnfa*) in mice from the indicated groups. Gene expression was normalized to *Actb* mRNA levels. n = 6 per group. (C) Expression of p-IKKβ, IKKβ, IKBα, p-p65, p65, and glyceraldehyde 3-phosphate dehydrogenase (GAPDH) was analyzed by western blotting. GAPDH served as a loading control. n = 3 per group. (D) Representative histological images of liver sections were examined by PSR staining. n = 6 per group. Scale bar, 100 μm. (E) Quantitative PCR was performed to determine hepatic mRNA levels of genes related to fibrosis indicators (*Col1a1*, *Col3a1*, *Ctgf*, and *Timp1*) in mice from the indicated groups. Gene expression was normalized to *Actb* mRNA levels. n = 6 per group. The data are presented as the mean ± SD. *Significant difference between the control-HFHC group and the breviscapine-HFHC group, *p < 0.05, **p < 0.01. The data were analyzed with one-way ANOVA. Abbreviations: Bre, breviscapine; HPF, high-power field

Breviscapine attenuates lipid accumulation and inflammation in hepatocytes

Primary hepatocytes are considered to be the primary cell type of the liver architecture and the major cells responsible for metabolic disorders. Next, we investigated the effects of breviscapine (50 and 100 μM) on lipid accumulation and inflammation in primary hepatocytes and L02 hepatocytes treated with palmitic acid (PA) + oleic acid (OA; = PO). Lipid accumulation (assayed by oil red O staining) (Figure 5A,B) and hepatic TG (Figure 5C) and TC (Figure S3) levels were significantly increased in primary hepatocytes and L02 hepatocytes treated with PO. However, the induction of lipid accumulation in primary hepatocytes and L02 hepatocytes was blunted by breviscapine treatment (Figure 5A–C). Furthermore, breviscapine treatment reduced the

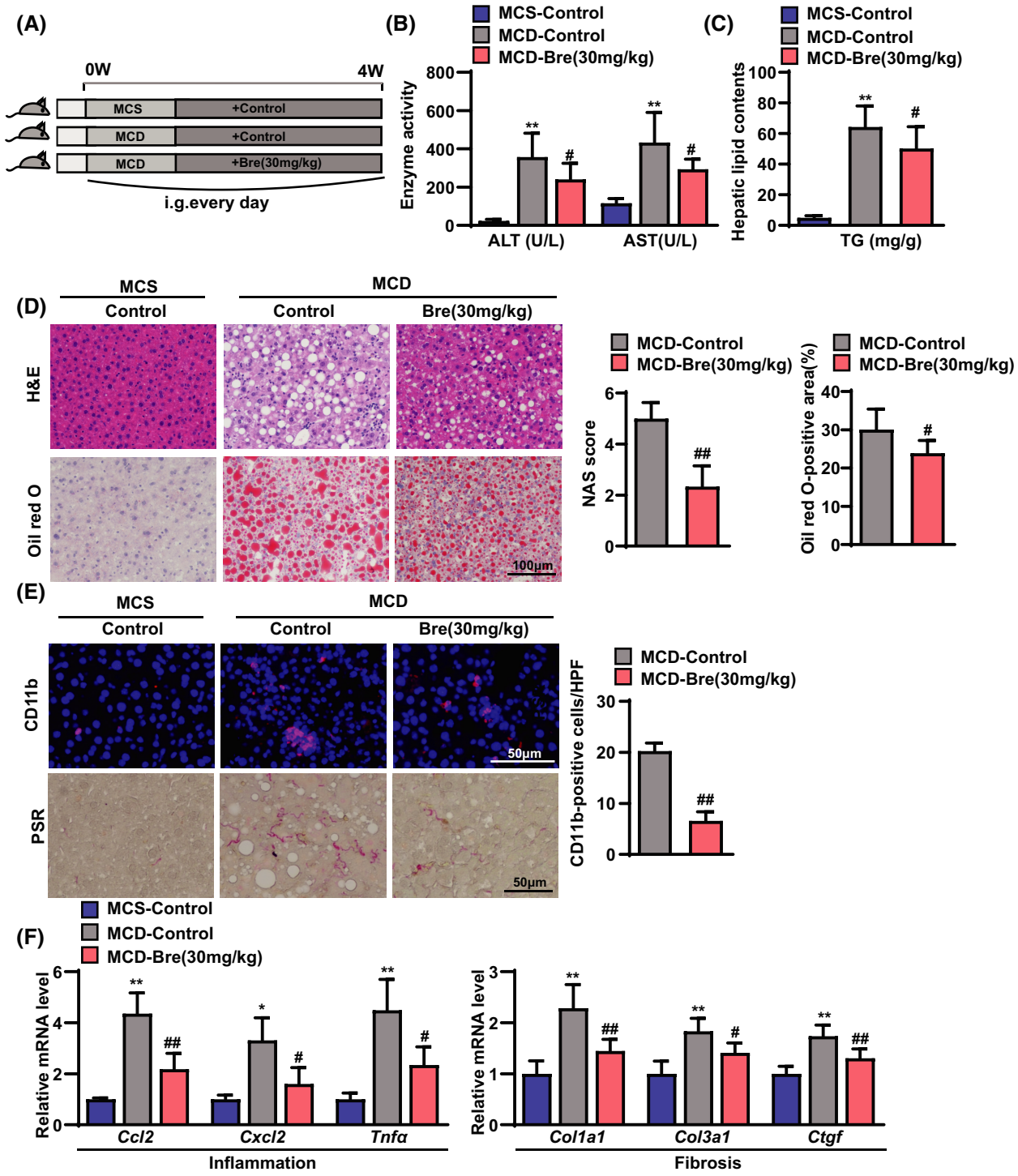

FIGURE 4 Breviscapine suppresses hepatic steatosis, inflammation, and fibrosis in mice fed an MCD diet. (A) Schematic diagram of the experimental procedure used to examine the protective effects of breviscapine in mice fed a methionine- and choline-sufficient (MCS) or MCD diet for 4 weeks. MCD diet–fed mice were intragastrically administered saline or breviscapine (15 or 30 mg/kg) once daily for 4 weeks. n = 12–15 per group. (B) Serum levels of ALT and AST measured in mice after 4 weeks of MCD diet challenge. n = 12–15 per group. (C) Liver lipid (TG) levels. n = 10–15 per group. (D) Representative images of hepatic steatosis and lipid accumulation stained with H&E and oil red O. NAFLD activity scores and the ratios of oil red O–positive areas are shown. n = 6 per group. Scale bar, 100 μm. (E) Immunofluorescence staining of CD11b (in red) and representative histological images stained with PSR in liver sections from the indicated mice after MCD diet challenge. Nuclei were labeled with DAPI (in blue). The ratios of the numbers of CD11b-positive cells are shown. n = 4 per group. Scale bar, 50 μm. n = 6 mice per group. Scale bar, 50 μm. (F) Quantitative PCR was performed to determine the hepatic mRNA levels of genes related to inflammation (*Ccl2*, *Cxcl2*, and *Tnfa*) and fibrosis indicators (*Col1a1*, *Col3a1*, and *Ctgf*) in the liver samples of control-MCS, control-MCD, and breviscapine (30 mg/kg)-MCD mice. Gene expression was normalized to *Actb* mRNA levels. n = 5 per group. The data are presented as the mean ± SD. Significant difference between the control-MCS group and the control-MCD group, $^{*}p < 0.05$, $^{**}p < 0.01$; significant difference between the control-MCD group and the breviscapine-MCD group, $^{\#}p < 0.05$, $^{\#\#}p < 0.01$. The data were analyzed with one-way ANOVA or two-tailed Student t test. Abbreviations: Bre, breviscapine; HPF, high-power field; i.g., intragastric administration; NAS, NAFLD activity score

mRNA levels of the lipogenic genes *Fasn*, *Scd1*, and acetyl CoA carboxylase alpha (*Acc*α) in PO-treated primary hepatocytes (Figure 5D). In addition, the expression of proinflammatory genes (*Cxcl10*, *Tnf*α, and *Ccl2*) was significantly decreased by breviscapine in primary hepatocytes cultured in PO medium (Figure 5E). Similar results from the quantitative PCR assay were observed in L02 hepatocytes cultured with PO in the absence or presence of breviscapine (Figure 5D,E). Together, these data indicate that breviscapine attenuates steatohepatitis changes in hepatocytes.

Breviscapine prevents NASH by systematically blunting the pathways involved in lipid metabolism, inflammation, fibrosis, and apoptosis

To systemically elucidate how breviscapine prevents NASH, we performed RNA-seq on the livers of HFHC diet–fed mice treated with breviscapine. Unsupervised PCA and hierarchical clustering clearly separated the samples from the control mice fed the HFHC diet and the breviscapine-treated mice fed the HFHC diet into two clusters (Figure 6A). GSEA revealed that genes related to lipid metabolism, inflammation, fibrosis, and apoptosis were enriched (Figure 6B) and significantly down-regulated by breviscapine treatment (Figure 4A). Moreover, a heatmap based on GSEA indicated that hepatic genes involved in lipid metabolism, inflammation, fibrosis, and apoptosis pathways were significantly down-regulated by breviscapine treatment in mice fed the HFHC diet for 16 weeks *in vivo* (Figure 6C).

Furthermore, we performed RNA-seq analysis on PO-treated L02 cells treated with breviscapine *in vitro*. PCA and hierarchical clustering clearly separated the samples from the breviscapine-treated group and the DMSO-control group (Figure S5A). The GSEA results showed that the lipid metabolism–related, inflammation-related, and apoptosis-related pathways were mainly enriched (Figure S5B,C) and that genes were significantly down-regulated by breviscapine treatment compared with DMSO treatment (Figure S6). Collectively, these results demonstrate that breviscapine treatment protects against NASH by suppressing hepatic damage, steatosis, inflammation, and fibrosis under conditions of metabolic stress.

Breviscapine inhibits the mitogen-activated protein kinase pathway in hepatocytes and liver tissue under metabolic stress

To investigate the molecular mechanism(s) underlying the anti-NASH effect of breviscapine, the transcriptomes of breviscapine-treated hepatocytes treated with PO and mice fed the HFHC diet were combined and analyzed by KEGG analysis and GSEA (Figure 7A). Subsequently, we analyzed the data in combination with the transcriptomes of cells and mice and found that a total of nine signaling pathways were enriched at the cellular level, while five signaling pathways were enriched at the tissue level. Through Venn analysis, we found that breviscapine treatment affected two identical signaling pathways *in vitro* and *in vivo*: the mitogen-activated protein kinase (MAPK) signaling pathway and the TGF-β signaling pathway (Figure 7B). Moreover, the gene numbers of the MAPK signaling pathway were greater than those of the TGF-β signaling pathway (Figure 7B). Subsequently, proteomic analysis showed that differential proteins related to lipid metabolism and inflammation were highly enriched in mice fed the HFHC diet but significantly down-regulated by breviscapine treatment (Figure 7C,D).

To uncover the key effector(s) that contributes to breviscapine-induced protection from NASH, we integrated the results from proteomic analysis, phosphoproteomic analysis, and transcriptomic characterization. We found a strong correlation between the DEGs and the differentially phosphorylated MAPK signaling molecules under breviscapine treatment, as illustrated by the STRING protein interaction network database (Figure 7E). Furthermore, MAPK14, heat shock protein A8, and MAP3K7 were the top 3 phosphoproteins according to the protein–protein interaction (PPI) degree (Figure 7F). MAPK14 is a member of the MAPK family. MAPK signaling is integrally involved in various physiological processes, such as inflammation, apoptosis, oxidative stress, and fibrotic responses.[15] TAK1 is a MAP3K protein and has been defined as a critical upstream molecule of MAPKs.[16] Thus, to further investigate whether breviscapine protects against NASH by regulating the MAPK signaling pathway, western blotting was used to analyze the activation of MAPK signaling *in vitro* and *in vivo*. The phosphorylation of TAK1, c-Jun N-terminal kinase (JNK), and p38 was significantly suppressed by breviscapine treatment after PA, HFD, or HFHC diet treatment (Figure 7G). These data suggest that breviscapine inhibits TAK1 and its downstream signaling pathway in hepatocytes or livers subjected to metabolic stress.

TAK1 inhibition is required for the breviscapine-induced suppression of lipid accumulation and the proinflammatory response in hepatocytes

To verify whether inhibition of TAK1-dependent signaling is required for the anti-NASH effects of breviscapine, we used 5Z-7-oxozeaenol, which is

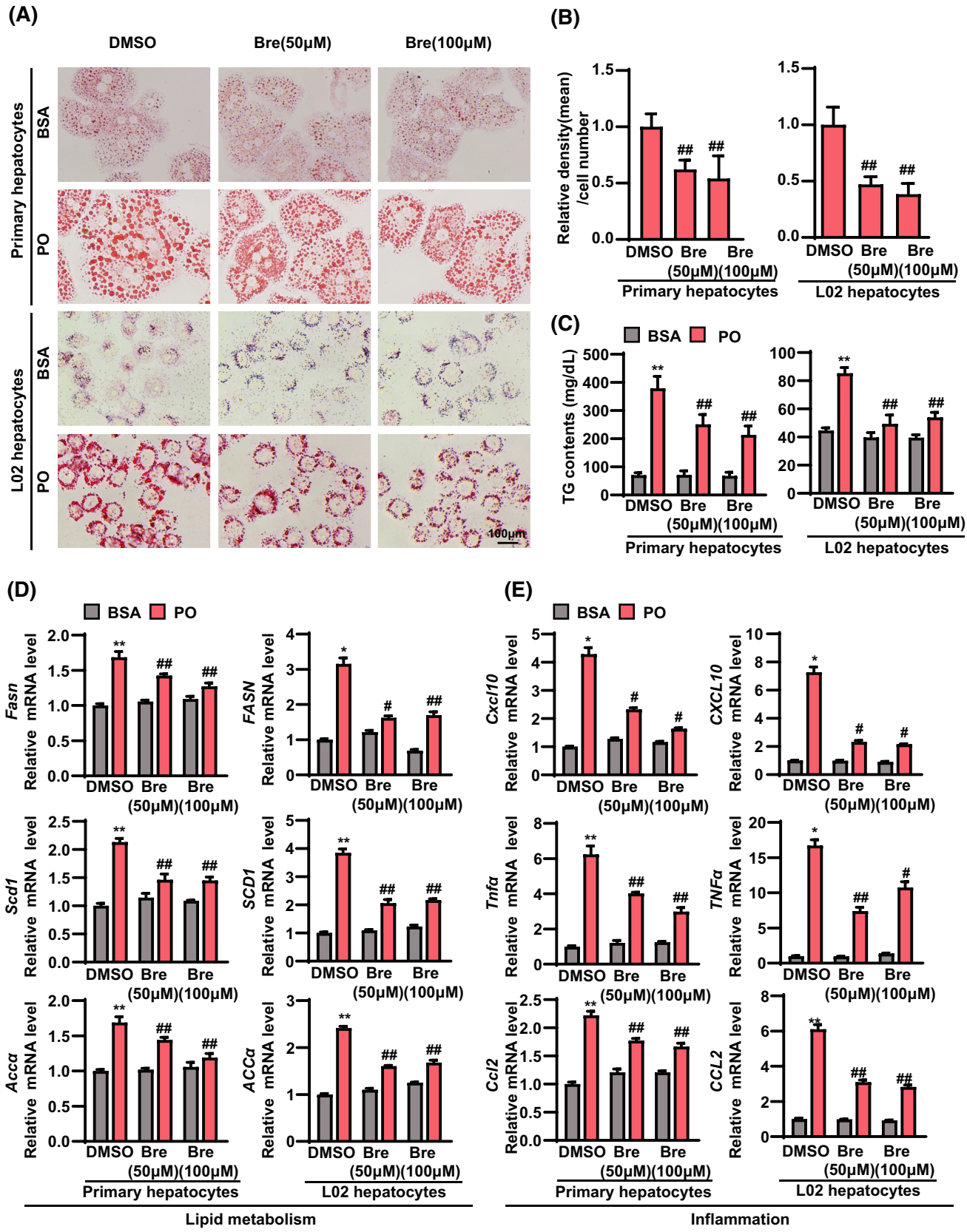

a potent irreversible selective inhibitor of TAK1. 5Z-7-Oxozeaenol prevents inflammation by inhibiting the catalytic activity of TAK1 MAPK kinase kinase.[17] Notably, oil red O staining showed that 5Z-7-oxozeaenol pretreatment almost completely abrogated the reduction in lipid accumulation induced

FIGURE 5 Breviscapine reduces lipid accumulation and inflammation in primary hepatocytes and L02 cells treated with PO. Primary hepatocytes were cultured in PO medium containing 0.2 mM PA and 0.4 mM OA for 12 h. L02 cells were cultured in PO medium containing 0.5 mM PA and 1.0 mM OA for 12 h. (A) Representative oil red O staining images of primary hepatocytes and L02 cells stimulated with PO and treated with breviscapine (50 and 100 μM) for 12 h. Scale bar, 100 μm. $n = 3$ independent experiments per group. (B) Quantitative analysis of oil red O staining in hepatocytes. (C) Levels of TGs and TC in primary hepatocytes and L02 cells in the indicated groups. The data were obtained from three independent experiments per group. (D) mRNA levels of genes related to lipid metabolism (*Fasn*, *Scd1*, and *Acc*α) and (E) inflammation (*Cxcl10*, *Tnf*α, and *Ccl2*) in primary hepatocytes and L02 cells in the indicated groups. Gene expression was normalized to *Actb* mRNA levels. The data were obtained from three independent experiments per group. The data are presented as the mean ± SD. Significant difference between the DMSO-bovine serum albumin group and the DMSO-PO group, $^{*}p < 0.05$, $^{**}p < 0.01$; significant difference between the DMSO-PO group and the breviscapine-PO group, $^{\#}p < 0.05$, $^{\#\#}p < 0.01$. The data were analyzed with one-way ANOVA. Abbreviations: Bre, breviscapine; BSA, bovine serum albumin

by breviscapine treatment in PO-treated hepatocytes (Figure 8A,B). In addition, breviscapine significantly decreased the intracellular TG and TC levels, while these effects were abolished by pretreatment with 5Z-7-oxozeaenol (Figure 8C). Furthermore, pretreatment with 5Z-7-oxozeaenol abolished the reductions in the expression of fatty acid synthesis genes (*Fasn*, *Scd1*, and *Acc*α) and proinflammatory genes (*Tnf*α, *Ccl2*, and *Cxcl10*) induced by breviscapine treatment (Figure 8D). Moreover, pretreatment with 5Z-7-oxozeaenol almost completely abrogated the breviscapine-induced phosphorylation of TAK1 and the downstream phosphorylation of JNK and p38 without changing the expression levels of total TAK1, JNK, and p38 in hepatocytes cultured with PA for 12 h (Figure 8E; Figure S7). Finally, we investigated the possibility of a direct interaction between breviscapine and TAK1. Because scutellarin, a prescription drug, is the main ingredient (≥90%) of breviscapine, we performed molecular docking of scutellarin with the TAK1 protein. Scutellarin exhibited suitable steric complementarity with the binding site of TAK1. Hydrogen bond interactions occurred between TAK1 and scutellarin. The oxygen atoms of scutellarin, regarded as hydrogen bond acceptors, formed hydrogen bonds with the backbone nitrogen atoms of Ala107 and Asp175. The nitrogen atom of scutellarin, regarded as a hydrogen bond donor, formed a hydrogen bond with the backbone oxygen atom of Ala107 (Figure 8F). These data suggest that inhibition of TAK1 is required for breviscapine to protect hepatocytes from PO-induced lipid accumulation and inflammation.

DISCUSSION

Exercise training and dietary interventions remain the primary recommendations for patients with NAFLD and its progressive stage, NASH.[18] However, for multiple societal, psychological, physical, genetic, and epigenetic reasons, it is challenging for patients to adhere to such lifestyle modifications; thus, pharmacotherapy for NAFLD, especially incurable NASH, is essential. Nevertheless, few medications are currently available to meet the increasing disease burdens of NAFLD and NASH.[19] Traditional Chinese medicine (TCM) has played a very large role in the prevention and treatment of NAFLD in China due to its unique theories on the etiology, pathogenesis, diagnosis, and treatment of fatty liver, such as the theories of *Tiao Gan Qi Shu Hua Zhuo* and the liver-based regulatory system for metabolic homeostasis.[20] In recent years, accumulating evidence has demonstrated the beneficial role of Chinese herbal medicine in the treatment of NAFLD.[12,21,22] Breviscapine has a wide range of pharmacological effects, such as antioxidative, anti-inflammatory, antifibrotic, and lipid-lowering effects (similar to the *Hua Zhuo* effect of TCM) and is clinically used for the treatment of diabetes, NAFLD, and other metabolic diseases.[23,24] These uses show that modern medicine and traditional medicine have the same understanding of these diseases. In this study, we discovered that breviscapine ameliorates NAFLD and NASH through suppression of the TAK1 signaling pathway.

Breviscapine, a mixture of flavonoid glycosides, has strong biological activity and is also a common monomeric compound used in clinical practice. It has been formulated into a variety of dosage forms for the treatment of cardiovascular and cerebrovascular diseases, such as atherosclerosis, coronary heart disease, and insufficient cerebral blood supply.[25] A clinical study has shown that breviscapine reduces hyperlipidemia in patients.[26] Additionally, breviscapine reduces hepatic lipid accumulation in HFD-fed rats[10] and mice.[27] Our results revealed that breviscapine significantly attenuated lipid accumulation in response to metabolic stress in both murine models and *in vitro* hepatocytes. Furthermore, our results confirmed that breviscapine abolished hepatic inflammation and fibrosis in a variety of animal models under metabolic stress. Aberrant lipid metabolism, steatosis, hepatic inflammation, apoptosis, and fibrosis are considered the major pathological factors promoting the progression of NAFLD.[28] Using an unbiased systemic analysis, we found that breviscapine largely decreased the expression of genes associated with lipid metabolism, inflammation, apoptosis, and fibrosis in mice fed an HFHC diet.

NAFLD is triggered by an excessive supply of nutrients. Most ingested fat is diverted to adipose tissue

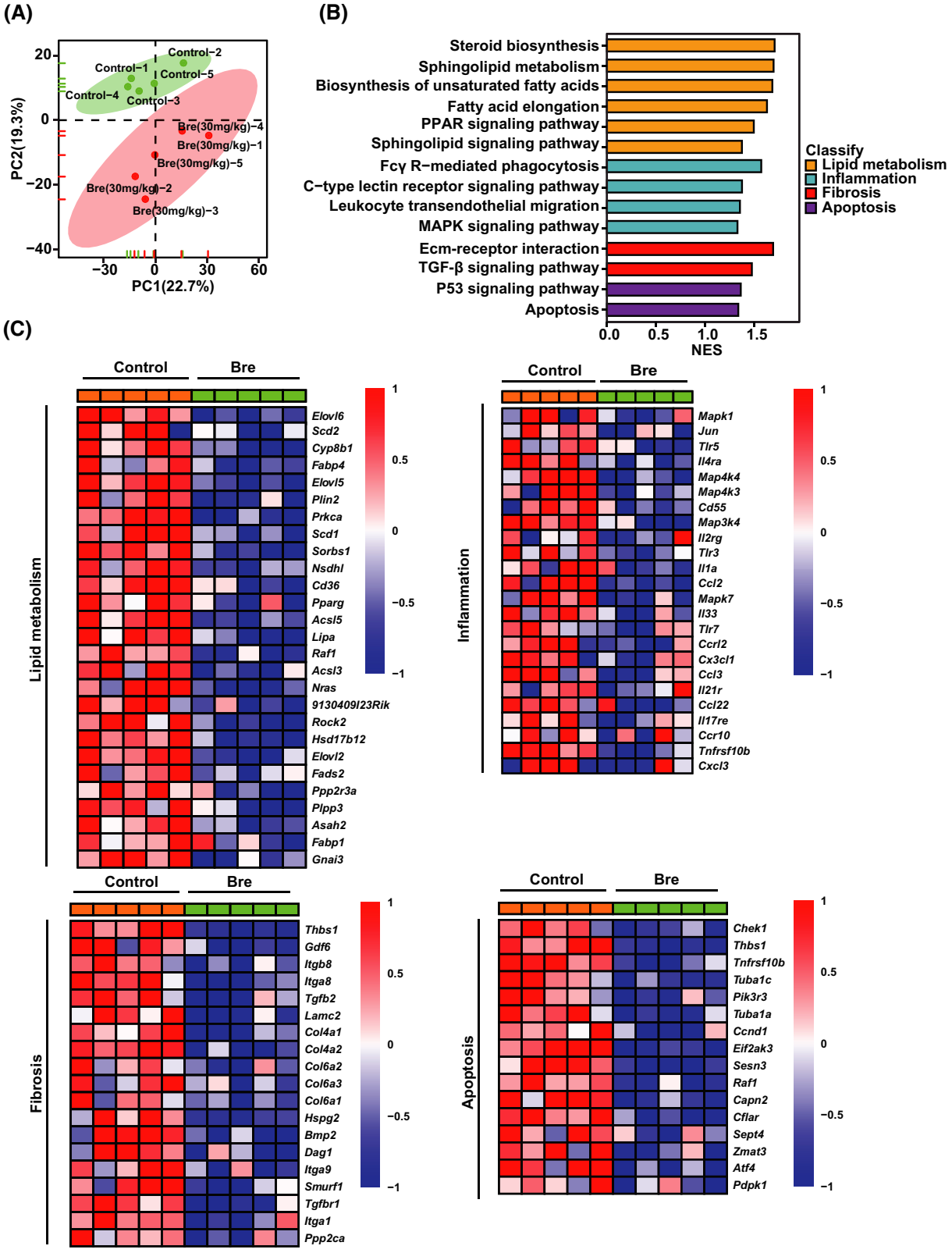

FIGURE 6 Transcriptomic analysis revealed the key differential targets in breviscapine-treated, HFHC diet–fed mice. (A) PCA of RNA-seq data from mice fed a control or HFHC diet for 16 weeks. *n* = 5 per group. (B) GSEA of pathways related to lipid metabolism, inflammation, fibrosis, and apoptosis. *n* = 5 per group. (C) Heatmaps of gene expression profiles related to lipid metabolism, inflammation, fibrosis, and apoptosis based on the RNA-seq data set. *n* = 5 per group. Abbreviations: Bre, breviscapine; Ecm, extracellular matrix; NES, normalized enrichment score; PC, principal component

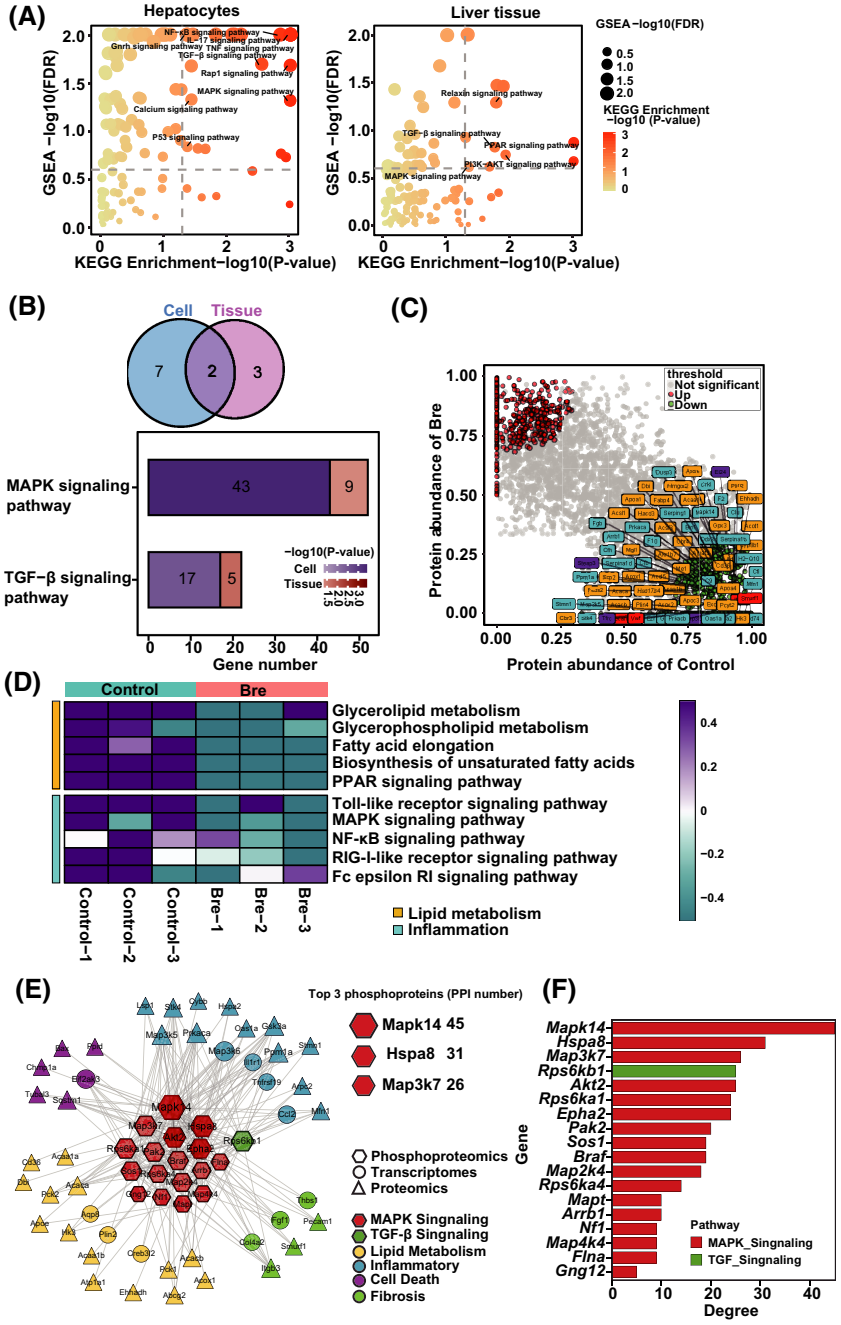

FIGURE 7 Multiomics analysis revealed that the MAPK pathway is the downstream target of breviscapine. (A) GSEA and KEGG pathway enrichment analysis of the transcriptomes of cells and HFHC diet–fed mouse liver samples. *n* = 3 independent experiments per group for cells, *n* = 5 per group for tissues. (B) Venn diagram of GSEA and KEGG pathway intersections based on transcriptome data both *in vivo* and *in vitro*. The histogram of the two key pathways is based on the corresponding scores. *n* = 3 independent experiments per group for cells, *n* = 5 per group for tissues. (C) Scatterplot showing the fold changes in all proteins in the proteomic data set, with differentially expressed proteins shown with corresponding font colors (inflammation in blue, lipid metabolism in yellow, fibrosis in red, apoptosis in purple). *n* = 3 per group. (D) Heatmap showing the degrees of influence of pathways related to lipid metabolism and inflammation based on a proteomic data set. *n* = 3 per group. (E) PPI network diagram of multiomics joint analysis. *n* = 3 per group. (F) Bar chart of phosphorylated proteins ranked according to PPI degree. *n* = 3 per group. (G) Western blot analysis of proteins involved in the MAPK signaling cascade in cells stimulated with PA and mice subjected to HFD or HFHC feeding. GAPDH served as a loading control. *n* = 3 per group. The data are presented as the mean ± SD. Significant difference between the DMSO/control group and the breviscapine group, $^{*}p < 0.05$, $^{**}p < 0.01$. The data were analyzed with one-way ANOVA. Abbreviations: Bre, breviscapine; FDR, false discovery rate; Hspa8, heat shock protein a8; RIG-I, retinoic acid–inducible gene I

or working muscle for storage or oxidation, but fat stored in white adipose tissue undergoes lipolysis to release fatty acids.[29] Excess fatty acids contribute to accumulation of very large amounts of TGs in hepatocytes and frequently lead to steatosis in the liver.[30] In this study, breviscapine reduced the hepatic lipid

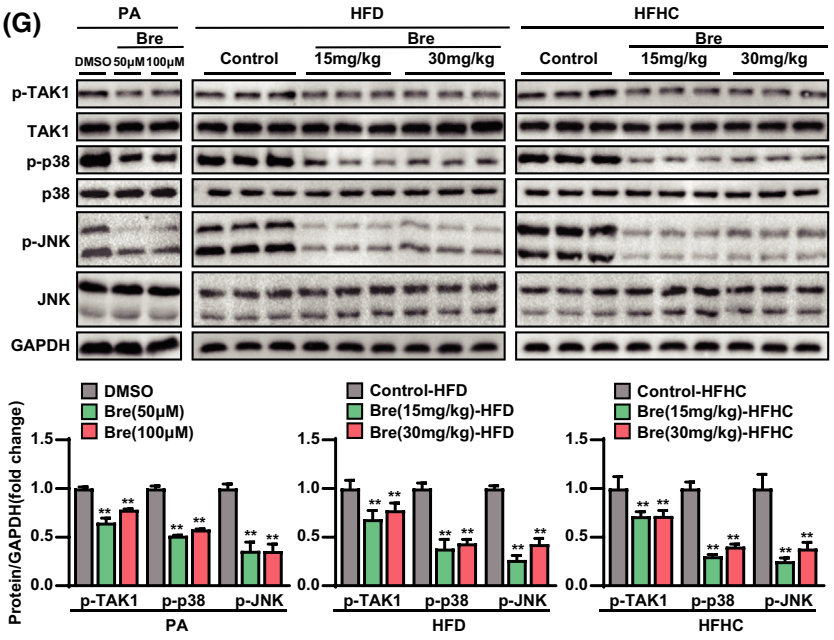

FIGURE 7 (Continued)

content in PO-treated hepatocytes and the livers of diet-induced mice. Moreover, breviscapine inhibited *Fasn*, *Acc*α, *Scd1*, *Cd36*, *Fabp1*, and *Ppar*γ mRNA expression and promoted *Ppar*α and *Cpt1*α mRNA expression *in vivo* and *in vitro*, suggesting that breviscapine may decrease hepatic lipid accumulation and steatosis by restraining *de novo* synthesis and uptake of fatty acids while accelerating fatty acid β-oxidation.

A characteristic of NASH is the presence of hepatic inflammation, and continued inflammation in the liver is thought to drive the development of fibrosis.[31] Previous studies have demonstrated that breviscapine inhibits lipopolysaccharide-induced production of proinflammatory mediators.[32] Recent studies have shown that the anti-inflammatory effects of breviscapine may be due to suppression of NF-κB and NLR family pyrin domain containing 3 inflammasome activation.[33,34] In the current study, breviscapine inhibited NF-κB signaling pathway activation and attenuated the secretion of proinflammatory cytokines under metabolic stress. Studies have shown that activation of NF-κBs, especially the NF-κB p65 subunit, is closely associated with collagen deposition in liver fibrosis.[35] In our study, genes associated with collagen production, such as *Col1a1*, *Col3a1*, *Ctgf*, and *Timp1*, were down-regulated by breviscapine in HFHC/MCD diet–induced murine models. In addition, analysis of PSR staining representing collagen deposition showed that breviscapine attenuated NASH-associated fibrosis.

To elucidate the possible mechanism by which breviscapine prevents NASH, a systematic analysis based on RNA sequence data was performed, and our data implicated MAPK signaling in the anti-NASH effects of breviscapine. The MAPK signaling pathway is involved in the regulation of inflammation and fatty acid metabolism.[36] TAK1 is an upstream kinase that activates NF-κB and MAPK signaling during NAFLD progression.[37] Due to the pivotal role of TAK1 in many physiological processes, such as inflammation, cell differentiation, and apoptosis, inhibition of TAK1 activation induced by metabolic stress may generate a potent hepatoprotective effect.[38] It has been demonstrated that inhibition of the long noncoding RNA HULC attenuates hepatic fibrosis and hepatocyte apoptosis by inhibiting the MAPK signaling pathway in rats with NAFLD.[39] Recent studies have pointed out the important roles of TAK1 in regulating hepatocyte lipid metabolism and reducing hepatocyte inflammation in NAFLD.[40,41] Restraining TAK1 activation attenuates hepatic steatosis, lipid deposition, and the inflammatory response in animals with HFD-induced NAFLD.[42–44] The results of the multiomics and western blot analyses further suggest that breviscapine inhibits TAK1 phosphorylation and downstream JNK/p38 activation, thereby postponing the pathogenesis of NASH. Our study demonstrates that breviscapine ameliorates NASH under metabolic stress conditions by regulating lipid metabolism, suppressing inflammation, and reducing liver fibrosis by specifically inhibiting TAK1 phosphorylation.

Collectively, our current findings demonstrate that breviscapine, identified as a specific inhibitor of TAK1, ameliorates the pathogenesis of NASH through suppression of hepatic lipid accumulation, inflammation, and fibrogenesis. Therefore, our findings will provide insights supporting the development of therapeutic approaches for NASH.

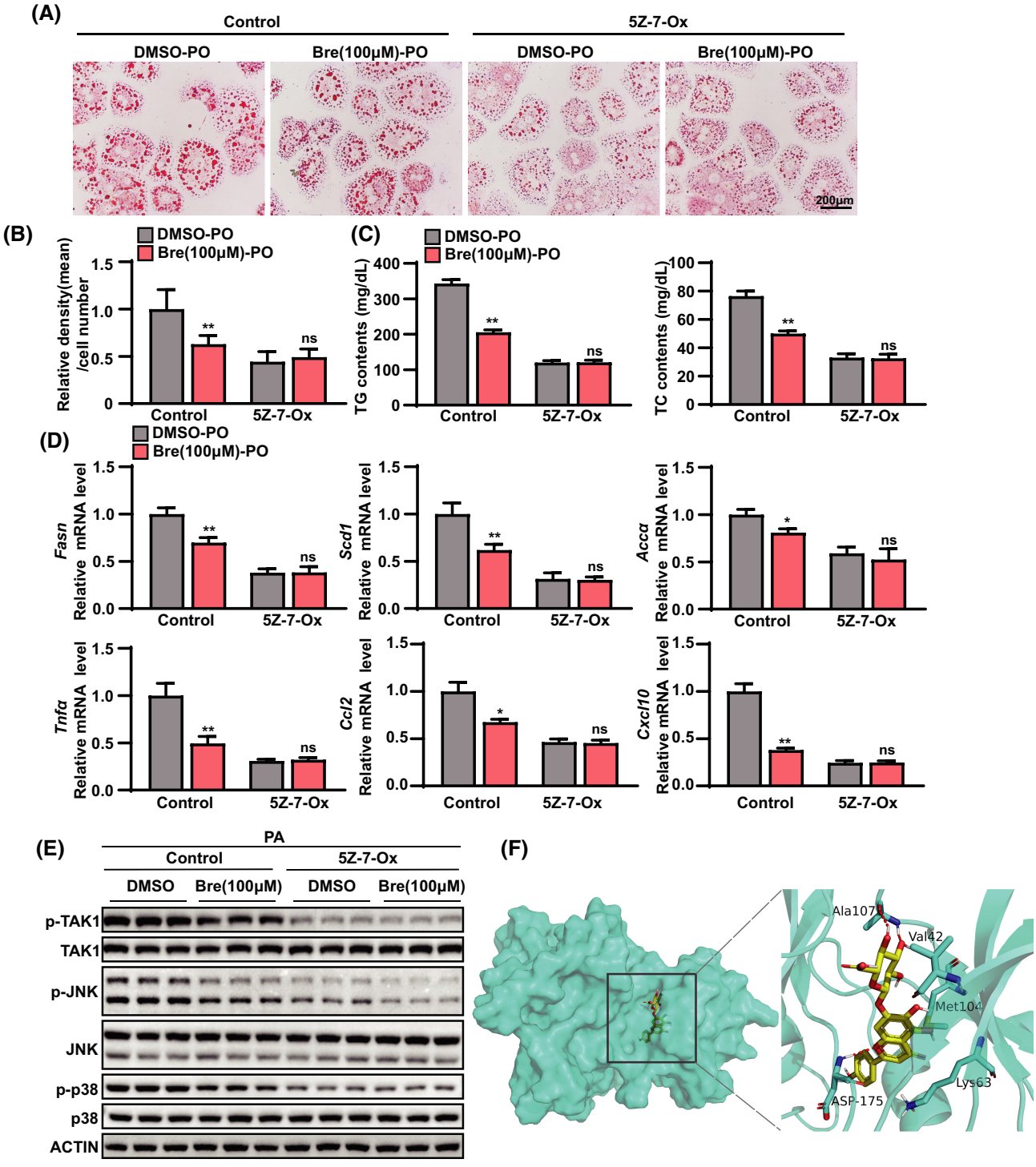

FIGURE 8 TAK1 inhibition is responsible for the effects of breviscapine on lipid accumulation and inflammation in hepatocytes. (A) Representative images of oil red O staining showing the degree of lipid accumulation in primary hepatocytes treated with DMSO or breviscapine (100 μM) after PO (0.2 mM PA and 0.4 mM OA) stimulation for 12 h in the presence or absence of 5Z-7-oxozeaenol (2 μM) for 12 h. Scale bar, 200 μm. The data were obtained from three independent experiments per group. (B) Quantitative analysis of the degree of lipid accumulation. (C) TG and TC levels in primary hepatocytes in the indicated groups stimulated with bovine serum albumin or PO (0.5 mM PA and 1.0 mM OA) for 12 h. Four independent experiments per group were performed. (D) Relative mRNA levels of inflammatory factors (*Tnfα*, *IL-1β*, and *Ccl10*) and lipogenic genes (*Fasn*, *Scd1*, and *Accα*) in primary hepatocytes treated with PO. The relative mRNA expression was normalized to that of the β-actin-encoding gene *Actb*. The data were obtained from three independent experiments per group. (E) Western blot analysis of total and phosphorylated protein levels of apoptosis signal–regulating kinase, JNK, and p38 protein in primary hepatocytes stimulated with PA for 12 h. Actin served as the loading control. The data were obtained from three independent experiments per group. (F) Molecular docking of breviscapine with the protein TAK1. The data are presented as the mean ± SD. Significant difference between the control-DMSO-PO group and the control-breviscapine-PO group, $*p < 0.05$, $**p < 0.01$. The data were analyzed with one-way ANOVA. Abbreviations: Bre, breviscapine; *ns*, no significant difference between the 5Z-7-oxozeaenol-DMSO-PO group and the 5Z-7-oxozeaenol-breviscapine-PO group; 5Z-7-Ox, 5Z-7-oxozeaenol

ACKNOWLEDGMENT

This work was supported by grants from the National Key R&D Plan of China "Research on Modernization of Traditional Chinese Medicine" program (2018YFC1704200), the National Natural Science Foundation of China (81830113, 81870420, and 82070590), the Major Basic and Applied Basic Research Projects in Guangdong Province of China (2019B030302005), and the Special Topics of General Projects of Guangzhou Science and Technology Plan of China (201904010075).

CONFLICT OF INTEREST

Nothing to report.

AUTHOR CONTRIBUTIONS

Conceptualization: Jiao Guo; Project administration: Jiao Guo; Funding acquisition: Jiao Guo, Tian Lan; Visualization: Tian Lan, Shuo Jiang, Jing Zhang, Qiqing Weng, Yang Yu, and Haonan Li; Writing – original draft: Tian Lan, Shuo Jiang, Jing Zhang, and Qiqing Weng; Writing – review & editing: Tian Lan, Shuo Jiang, Jing Zhang, Qiqing Weng, and Sha Hu; Investigation: Shuo Jiang, Jing Zhang, Qiqing Weng, Yang Yu, Haonan Li, and Song Tian; Data curation: Shuo Jiang, Jing Zhang, Qiqing Weng, Xin Ding, Yiqi Yang, Weixuan Wang, Lexun Wang, Duosheng Luo, Xue Xiao, Shenghua Piao, Qing Zhu, and Xianglu Rong; Supervision: Jiao Guo

ORCID

Tian Lan https://orcid.org/0000-0002-5783-6883

REFERENCES

1. Lin HY, Yang YL, Wang PW, Wang FS, Huang YH. The emerging role of microRNAs in NAFLD: highlight of microRNA-29a in modulating oxidative stress, inflammation, and beyond. Cells. 2020;9(4):1041.
2. Estes C, Razavi H, Loomba R, Younossi Z, Sanyal AJ. Modeling the epidemic of nonalcoholic fatty liver disease demonstrates an exponential increase in burden of disease. Hepatology. 2018;67:123–33.
3. Jian C, Fu J, Cheng XU, Shen L-J, Ji Y-X, Wang X, et al. Low-dose sorafenib acts as a mitochondrial uncoupler and ameliorates nonalcoholic steatohepatitis. Cell Metab. 2020;31:892–908.e11.
4. Liu W, Baker RD, Bhatia T, Zhu L, Baker SS. Pathogenesis of nonalcoholic steatohepatitis. Cell Mol Life Sci. 2016;73:1969–87.
5. Villanueva MT. Liver disease: conscious uncoupling in NASH. Nat Rev Drug Discov. 2017;16:238–9.
6. Pengyue Z, Tao G, Hongyun H, Liqiang Y, Yihao D. Breviscapine confers a neuroprotective efficacy against transient focal cerebral ischemia by attenuating neuronal and astrocytic autophagy in the penumbra. Biomed Pharmacother. 2017;90:69–76.
7. Liu X, Cheng J, Zhang G, Ding W, Duan L, Yang J, et al. Engineering yeast for the production of breviscapine by genomic analysis and synthetic biology approaches. Nat Commun. 2018;9:448.
8. Wang L, Ma Q. Clinical benefits and pharmacology of scutellarin: a comprehensive review. Pharmacol Ther. 2018;190:105–27.
9. Liu Y, Wen PH, Zhang XX, Dai Y, He Q. Breviscapine ameliorates CCl_4 induced liver injury in mice through inhibiting inflammatory apoptotic response and ROS generation. Int J Mol Med. 2018;42:755–68.
10. Fan H, Ma X, Lin P, Kang Q, Zhao Z, Wang L, et al. Scutellarin prevents nonalcoholic fatty liver disease (NAFLD) and hyperlipidemia via PI3K/AKT-dependent activation of nuclear factor (erythroid-derived 2)-like 2 (Nrf2) in rats. Med Sci Monit. 2017;23:5599–612.
11. Zhang X, Ji R, Sun H, Peng J, Ma X, Wang C, et al. Scutellarin ameliorates nonalcoholic fatty liver disease through the PPARgamma/PGC-1alpha-Nrf2 pathway. Free Radic Res. 2018;52:198–211.
12. Lan T, Yu Y, Zhang J, Li H, Weng Q, Jiang S, et al. Cordycepin ameliorates nonalcoholic steatohepatitis via activation of AMP-activated protein kinase signaling pathway. Hepatology 2021;74:686–703.
13. Weiß J, Rau M, Geier A. Non-alcoholic fatty liver disease. Deutsches Aerzteblatt. 2014;111:447–52.
14. Gong J, Fang C, Zhang P, Wang P-X, Qiu Y, Shen L-J, et al. Tumor progression locus 2 in hepatocytes potentiates both liver and systemic metabolic disorders in mice. Hepatology. 2019;69:524–44.
15. Kyriakis JM, Avruch J. Mammalian MAPK signal transduction pathways activated by stress and inflammation: a 10-year update. Physiol Rev. 2012;92:689–737.
16. Skaug B, Jiang X, Chen ZJ. The role of ubiquitin in NF-kappaB regulatory pathways. Annu Rev Biochem. 2009;78:769–96.
17. Ninomiya-Tsuji J, Kajino T, Ono K, Ohtomo T, Matsumoto M, Shiina M, et al. A resorcylic acid lactone, 5Z-7-oxozeaenol, prevents inflammation by inhibiting the catalytic activity of TAK1 MAPK kinase kinase. J Biol Chem. 2003;278:18485–90.
18. Worm N. Beyond body weight-loss: dietary strategies targeting intrahepatic fat in NAFLD. Nutrients. 2020;12(5):1316.
19. Neuschwander-Tetri BA. Therapeutic landscape for NAFLD in 2020. Gastroenterology. 2020;158:1984–98.e83.
20. Guo J. Research progress on prevention and treatment of glucolipid metabolic disease with integrated traditional Chinese and Western medicine. Chin J Integr Med. 2017;23:403–9.
21. Yan T, Yan N, Wang P, Xia Y, Hao H, Wang G, et al. Herbal drug discovery for the treatment of nonalcoholic fatty liver disease. Acta Pharm Sin B. 2020;10:3–18.
22. Chen YU, He X, Yuan X, Hong J, Bhat O, Li G, et al. NLRP3 inflammasome formation and activation in nonalcoholic steatohepatitis: therapeutic target for antimetabolic syndrome remedy FTZ. Oxid Med Cell Longev. 2018;2018:2901871.
23. Chledzik S, Strawa J, Matuszek K, Nazaruk J. Pharmacological effects of scutellarin, an active component of genus *Scutellaria* and *Erigeron*: a systematic review. Am J Chin Med. 2018;46:319–37.
24. Gao L, Tang H, Zeng Q, Tang T, Chen M, Pu P. The anti-insulin resistance effect of scutellarin may be related to antioxidant stress and AMPKalpha activation in diabetic mice. Obes Res Clin Pract. 2020;14:368–74.
25. Yan F, Feng J, Li W, Wu L, Li J. A preliminary study on the effect and mechanism of breviscapine for improving insulin resistance in HepG2 cells. J Cardiovasc Pharmacol. 2020;76:216–26.
26. Gao J, Chen G, He H, Liu C, Xiong X, Li J, et al. Therapeutic effects of breviscapine in cardiovascular diseases: a review. Front Pharmacol. 2017;8:289.
27. Luan H, Huo Z, Zhao Z, Zhang S, Huang Y, Shen Y, et al. Scutellarin, a modulator of mTOR, attenuates hepatic insulin resistance by regulating hepatocyte lipid metabolism via SREBP-1c suppression. Phytother Res. 2020;34:1455–66.
28. Ross TT, Crowley C, Kelly KL, Rinaldi A, Beebe DA, Lech MP, et al. Acetyl-CoA carboxylase inhibition improves multiple dimensions of NASH pathogenesis in model systems. Cell Mol Gastroenterol Hepatol. 2020;10:829–51.
29. Zhao G-N, Tian Z-W, Tian T, Zhu Z-P, Zhao W-J, Tian H, et al. TMBIM1 is an inhibitor of adipogenesis and its depletion

promotes adipocyte hyperplasia and improves obesity-related metabolic disease. Cell Metab. 2021;33:1640–54.e48.
30. Machado MV, Diehl AM. Pathogenesis of nonalcoholic steatohepatitis. Gastroenterology. 2016;150:1769–77.
31. Schuster S, Cabrera D, Arrese M, Feldstein AE. Triggering and resolution of inflammation in NASH. Nat Rev Gastroenterol Hepatol. 2018;15:349–64.
32. Wang S, Wang H, Guo H, Kang L, Gao X, Hu L. Neuroprotection of scutellarin is mediated by inhibition of microglial inflammatory activation. Neuroscience. 2011;185:150–60.
33. Zhang L, Sun S, Li W, Zhang W, Wang X, Yang SY. Effect of scutellarin inhibits collagen-induced arthritis through TLR4/NFκB-mediated inflammation. Mol Med Rep. 2017;16:5555–60.
34. Li G, Guan C, Xu L, Wang L, Yang C, Zhao L, et al. Scutellarin ameliorates renal injury via increasing CCN1 expression and suppressing NLRP3 inflammasome activation in hyperuricemic mice. Front Pharmacol. 2020;11:584942.
35. Wang F, Liu S, Du T, Chen H, Li Z, Yan J. NF-kappaB inhibition alleviates carbon tetrachloride-induced liver fibrosis via suppression of activated hepatic stellate cells. Exp Ther Med. 2014;8:95–9.
36. Sun H, Wang X, Chen J, Song K, Gusdon AM, Li L, et al. Melatonin improves non-alcoholic fatty liver disease via MAPK-JNK/P38 signaling in high-fat-diet-induced obese mice. Lipids Health Dis. 2016;15:202.
37. Wu YK, Hu LF, Lou DS, Wang BC, Tan J. Targeting DUSP16/TAK1 signaling alleviates hepatic dyslipidemia and inflammation in high fat diet (HFD)–challenged mice through suppressing JNK MAPK. Biochem Biophys Res Commun. 2020;524:142–49.
38. Wang J, Ma J, Nie H, Zhang XJ, Zhang P, She ZG, et al. Hepatic regulator of G protein signaling 5 ameliorates NAFLD by suppressing TAK1-JNK/p38 signaling. Hepatology. 2020;73(1):104–25.
39. Shen X, Guo H, Xu J, Wang J. Inhibition of lncRNA HULC improves hepatic fibrosis and hepatocyte apoptosis by inhibiting the MAPK signaling pathway in rats with nonalcoholic fatty liver disease. J Cell Physiol. 2019;234:18169–79.
40. Ye P, Liu J, Xu W, Liu D, Ding X, Le S, et al. Dual-specificity phosphatase 26 protects against nonalcoholic fatty liver disease in mice through transforming growth factor beta-activated kinase 1 suppression. Hepatology. 2019;69:1946–64.
41. Wu L, Liu Y, Zhao Y, Li M, Guo L. Targeting DUSP7 signaling alleviates hepatic steatosis, inflammation and oxidative stress in high fat diet (HFD)–fed mice via suppression of TAK1. Free Radic Biol Med. 2020;153:140–58.
42. Liu Y, Song J, Yang J, Zheng J, Yang L, Gao J, et al. Tumor necrosis factor-α-induced protein 8-like 2 alleviates nonalcoholic fatty liver disease via suppressing TAK1 activation. Hepatology 2021;74:1300–18.
43. Ji Y-X, Huang Z, Yang X, Wang X, Zhao L-P, Wang P-X, et al. The deubiquitinating enzyme cylindromatosis mitigates nonalcoholic steatohepatitis. Nat Med. 2018;24:213–23.
44. Liu D, Zhang P, Zhou J, Liao R, Che Y, Gao M-M, et al. TNFAIP3 interacting protein 3 overexpression suppresses nonalcoholic steatohepatitis by blocking TAK1 activation. Cell Metab. 2020;31:726–40.e28.

SUPPORTING INFORMATION

Additional supporting information may be found in the online version of the article at the publisher's website.

How to cite this article: Lan T, Jiang S, Zhang J, Weng Q, Yu Y, Li H, et al. Breviscapine alleviates NASH by inhibiting TGF-β-activated kinase 1-dependent signaling. Hepatology. 2022;76:155–171. doi:10.1002/hep.32221